

Recent Developments on Resolution and Applicability of Capillary Hydrodynamic Fractionation (CHDF)

J. Gabriel DosRamos, Matec Applied Sciences, 56 Hudson St.,
Northborough, MA 01532 USA

Abstract

Capillary Hydrodynamic Fractionation (CHDF) is a high-resolution particle size distribution (PSD) analysis technique. CHDF is used to measure the PSD of colloids in the particle size range of 5 nm to 3 microns.

CHDF fractionation occurs as an eluant or carrier fluid carries the particles downstream in a capillary tube. Large particles exit the fractionation capillary ahead of smaller particles. Particle fractionation occurs because of the combination of the eluant parabolic velocity profile (laminar flow), size exclusion of the particles at the capillary wall, and colloidal forces.

The aim of this study was to expand CHDF's applicability to a broader class of colloidal systems. This can widen CHDF's usefulness as a particle sizing technique.

Introduction

Particle sizing techniques can be grouped into High-Resolution (Fractionation) and Ensemble techniques (1). High-Resolution (HR) techniques are characterized by the fact that particles are fractionated according to size and/or mass during particle size analysis. Ensemble techniques perform measurements on all particles simultaneously without physical separation. HR particle size analyzers include Capillary Hydrodynamic Fractionation (CHDF), Field-Flow Fractionation, Single-Particle Counting, and Disc Centrifugation. Ensemble techniques include Laser Diffraction, Photon-Correlation Spectroscopy (PCS), acoustic-attenuation spectroscopy, and Turbidimetry. Electron Microscopy is in a class by itself as it offers high resolution but particles are not fractionated during analysis.

HR techniques offer a strong advantage in that they produce *true* particle size distribution (PSD) data. HR-based devices can in principle detect the presence of multiple particle size populations without making significant assumptions. On the other hand, HR devices tend to be more complicated to operate than ensemble instruments. Ensemble instruments produce mainly mean particle size and standard deviation data. Any mean particle size value can be produced by an

infinite number of PSD curves. This ill-conditioned problem, along with the fact that calculated PSD's vary significantly with minor noise in the raw data, force most ensemble devices to assume *a priori* the shape of the PSD (2). Despite these issues, ensemble devices are much more widely used than HR instruments. The two main reasons seem to be the following. Ensemble instruments are easier to use, and are more widely applicable to different types of dispersion/colloidal samples.

Figure 1 describes the particle size-based fractionation process in CHDF. Larger particles exit the fractionation open capillary ahead of smaller ones (3). A UV-detector is typically used as a particle-concentration detector. Such particle fractionation occurs because of a particle-size exclusion effect, plus colloidal forces affecting the particle motion. The latter consist mainly of particle/capillary electric double layer repulsion, and a lift force exerted by the moving fluid on the particles (4).

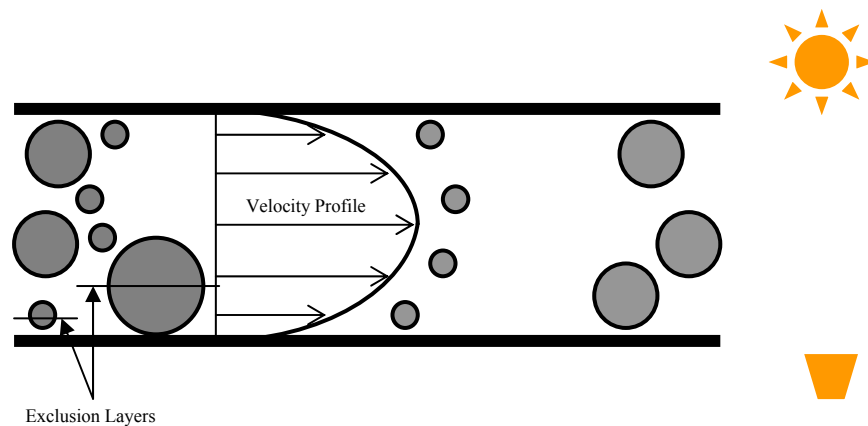


Figure 1. Particle size-based fractionation in CHDF.

Figure 2 shows CHDF2000 PSD data from two different polystyrene samples with the same volume-average mean particle size value of 226 nm even though their PSD's are noticeably different. This data exemplifies the risks of relying exclusively on mean particle size data. These samples will behave differently despite their identical mean particle size.

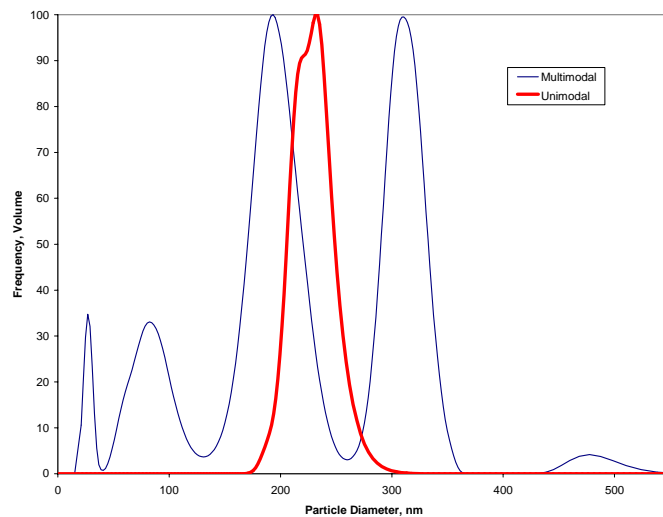


Figure 2. Two different samples analyzed by CHDF. Both have the same Volume-average (mean) particle size of 226 nm even though the PSD's are different.

It is in principle possible for a sample with a 226 nm mean particle size not to contain any 226 nm particles. This constitutes another disadvantage of relying on mean particle size data alone.

This paper describes efforts to expand the applicability of CHDF to different types of dispersed systems, including expanding its particle size analysis range. Also, a process on-line CHDF setup with automated sample dilution is presented.

Experimental

CHDF measurements were performed using a commercial CHDF2000 high-resolution particle size analyzer from Matec Applied Sciences, Northborough, MA (5). Various colloidal samples were used. Polystyrene samples were obtained from Duke Scientific (Indianapolis, IN), and Seradyn (Indianapolis, IN).

Nanoparticle Size Analysis

Small particles, especially under 50 nm, are becoming more widely manufactured and employed in various intermediate and final colloidal products. Accurate particle size analysis of these small particles is essential. Small particles offer a large total surface area. Secondary smaller particle size populations can be unexpectedly present in any dispersion. Such smaller particles can sharply influence the performance of any dispersion. Additionally, a small number of larger particles can pose difficulties, e.g., larger particles in inkjet printing inks can plug ink conduits in today's inkjet printers.

Particle sizing of nanoparticles is difficult for most particle sizing techniques. Because of refractive index issues, as well as the fact that larger particles mask smaller particles, ensemble-type measurements such as Laser Diffraction and Photon Correlation Spectroscopy (PCS) have difficulty analyzing such nanoparticles. High-resolution devices such as disc centrifuges are also limited due to the lack of tendency of nanoparticles to sediment, even under strong centrifugal fields.

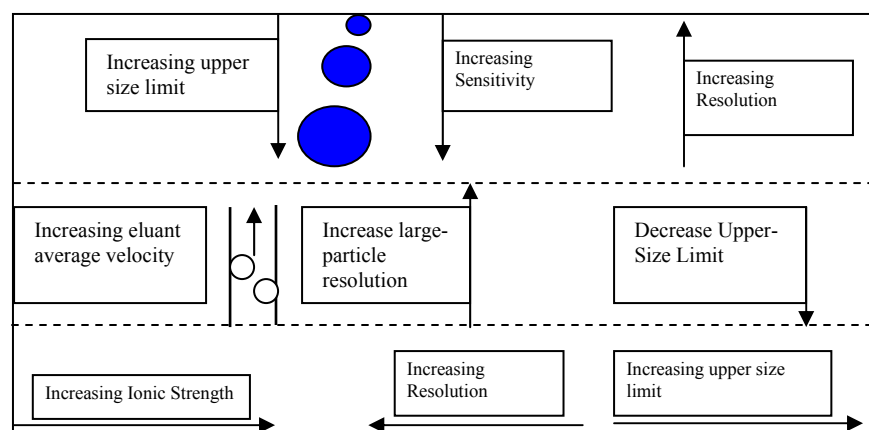


Figure 3. Effects of capillary inner diameter and eluant ionic strength and average velocity on CHDF resolution and particle size fractionation range.

Fig. 3 illustrates the effects of capillary ID, eluant average velocity, and eluant ionic strength on the resolution and particle-size fractionation range. As the capillary ID increases, so does the sample volume in the capillary. This increase in sample volume is due to the fact that the waste/fractionation split ratio changes (6), i.e. more sample flows into the fractionation capillary relative to the “waste” stream. Such increase in fractionated-sample volume results in stronger

particle detection in the CHDF particle-concentration detector, usually a UV detector.

Conversely, fractionation resolution increases as the capillary ID is reduced (7). This is due to several compounding factors as follows: (i) the particle exclusion layer is larger relative to the capillary ID, (ii) the lift force is stronger, and (iii) the particle fractograms are narrower due to lower axial dispersion.

The upper particle size limit decreases with decreasing capillary ID. Physically, larger particles can flow in a larger-ID fractionation capillary; also, the lift force is lower for larger-ID capillaries; this allows fractionation among larger particles.

The eluant average velocity also plays a role on the resolution and particle size range. As the eluant average velocity is increased, large-particle size fractograms become narrower. This Fractogram narrowing is due to the increase in lift force strength which forces larger particles to travel closer together. As the lift force increases, the upper particle size fractionation limit decreases similarly to reducing the capillary ID (8).

Suitable capillary ID and length, plus the eluant ionic strength and mean velocity can be combined to produce high resolution PSD data as shown in figures 4 and 5. Data is shown for the fractionation of eight particle size populations in less than 10 minutes.

This blend is composed of (from left to right on the raw-data graph) 800, 605, 420, 310, 240, 150, 60, and 20 nm. The peak separation on the raw data graph can be enhanced further by simply lengthening the fractionation time. The raw data peaks appear more overlapped than on the PSD. The reason is that a deconvolution procedure has been applied in the PSD computations (9). The deconvolution computations are similar to those used in Gel Permeation Chromatography for incorporating into the PSD computations axial dispersion of particles during capillary flow. Axial dispersion broadens the Fractogram width.

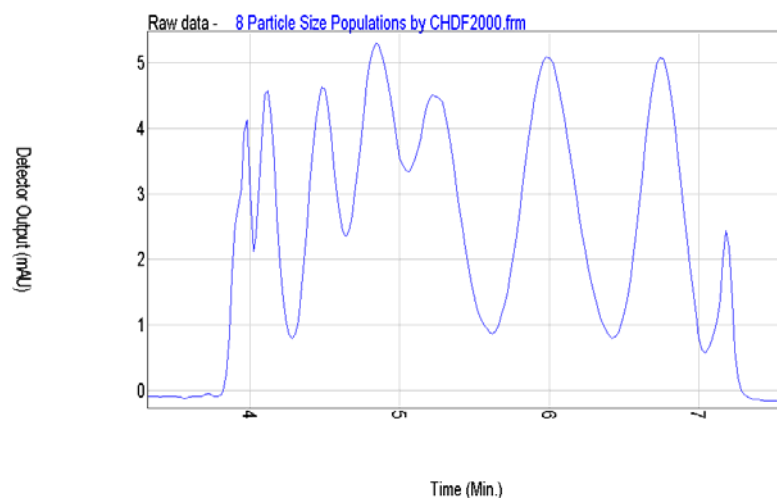


Figure 4. CHDF fractionation UV-detector raw data for a blend of 8 polystyrene calibration standards.

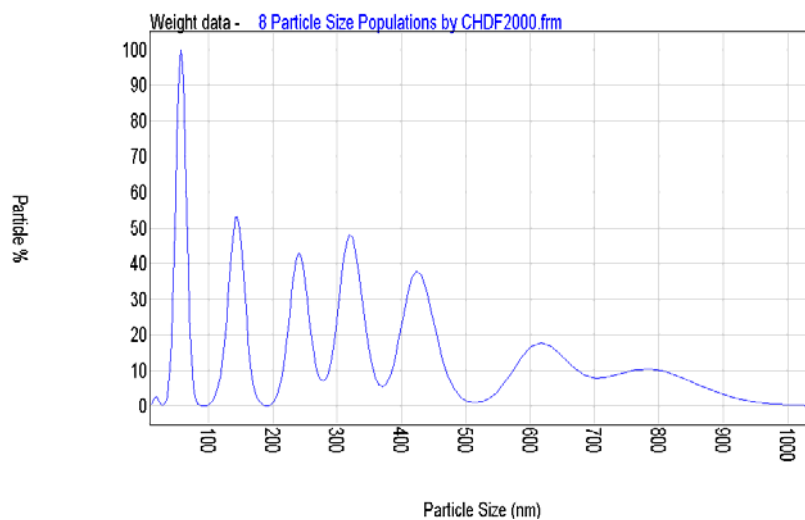


Figure 5. CHDF PSD data for an 8-mode polystyrene blend.

CHDF offers a useful alternative for nanoparticle analysis due to the fact that larger particles do not mask the presence of small particles, as well as, nanoparticle analysis is as easy and accurate as for larger particles. However, CHDF also faces difficulties in analyzing particles smaller than 20 nm. These

particles are difficult to quantify in the presence of larger particles due to large differences in UV-light extinction cross section (10). These difficulties are shown in the well-known Beer-Lambert's law equation as follows:

$$\text{D.O.} = N \text{ Rext } \chi \quad [1]$$

Where D.O. is the UV-detector output, N is the number of particles per unit volume, Rext is the particle extinction cross section, and χ is the UV-detector flow-cell path length. Equation [1] allows the calculation of N for each individual slice of particles exiting the CHDF fractionation capillary. N computations are susceptible to minor noise in D.O. when a sample contains particles under 20 nm along with larger particles, e.g. particles over 500 nm.

Figure 6 shows an extinction cross section curve for polystyrene particles in water. This curve was generated from Mie-theory computations built into the operating software on the commercial CHDF2000 device.

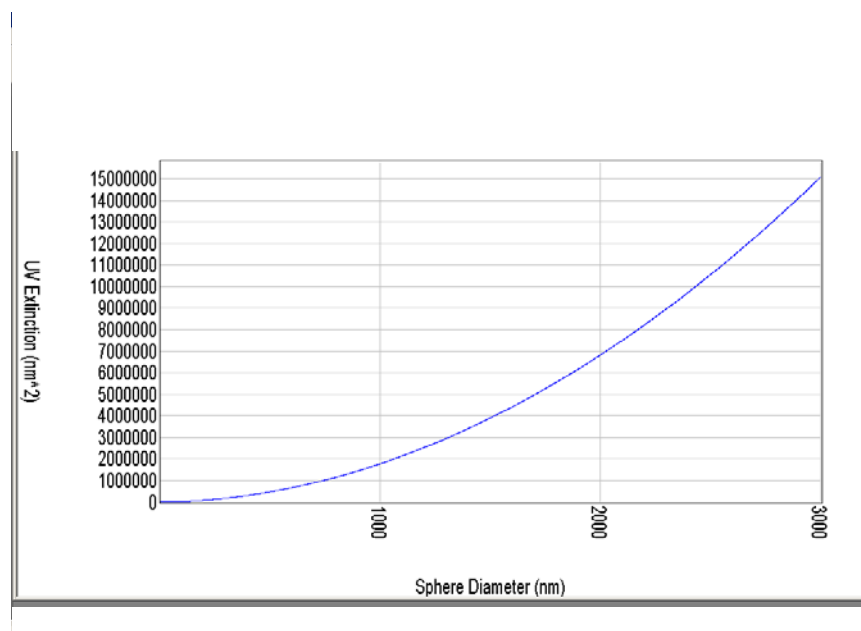


Figure 6. Extinction cross section for polystyrene particles in water. Curve generated from Mie theory computations.

Figure 6 shows that there are several orders of magnitude between the Rext of particles smaller than 20 nm and those larger than 500 nm. Consequently, small D.O. errors become largely amplified in the computation of N.

Despite the challenges described above, the CHDF2000 device was able to accurately perform particle sizing measurements of silica particles under 20 nm as shown in Figures 7 and 8.

The accurate measurement of these small particles was achieved by maximizing resolution and particle-detection sensitivity. This required optimizing the combination of suitable capillary diameter and length, and eluant ionic strength and average velocity.

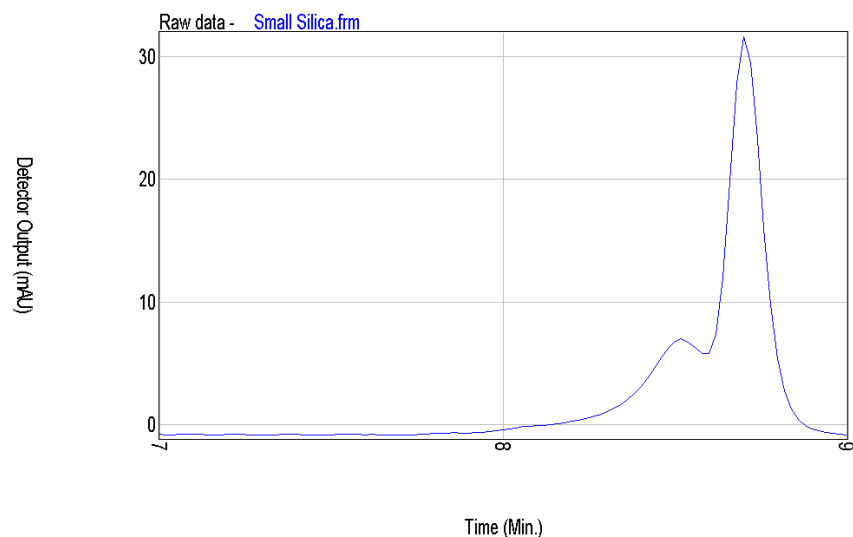


Figure 7. CHDF UV-detector raw data output for a 5-nm nominal particle size silica.

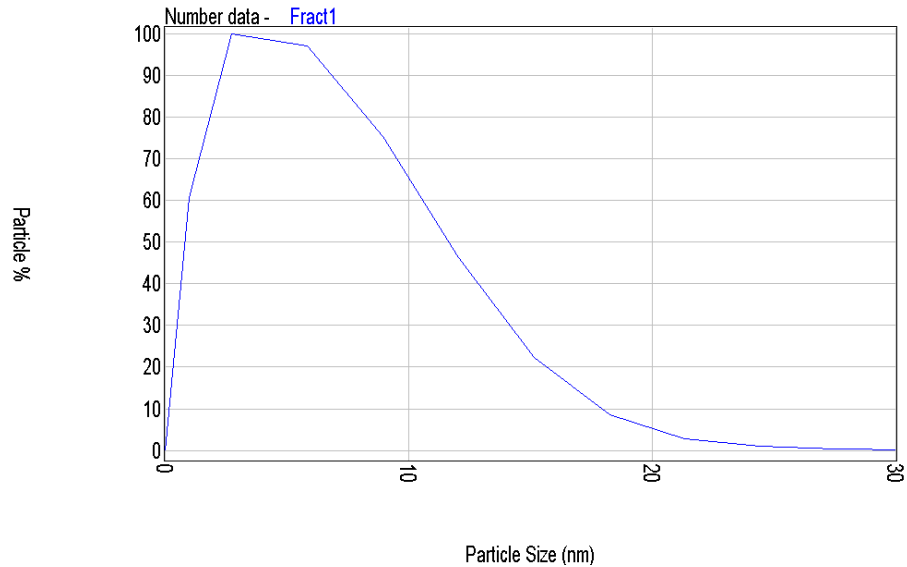


Figure 8. CHDF PSD for a 5-nm nominal particle size silica sample.

The CHDF raw data in figure 7 shows two main peaks located at 8.5 and 8.7 minutes. The peak at 8.7 minutes is believed to originate from UV-absorbing molecules in the sample such as surfactants, electrolytes, and acid or base molecules (11). These molecules exit the capillary last because their particle size is smaller than that of the silica particles. The molecular peak does not appear in the PSD graph of figure 8 because its particle size is below the low computational limit of 1 nm.

Figure 8 presents the PSD for this silica sample. A lognormal PSD shape is obtained ranging from 1 nm to 30 nm. The mode is located at 4 nm.

In order to achieve the maximum resolution required for these small particles (7) a low ionic strength (0.1 mM) carrier fluid was used in conjunction with a 5-micron ID fused silica capillary.

CHDF Particle Size Analysis of Micron-Sized Particles

CHDF has been commonly used for analysis of particles below 1 micron in size. As mentioned above, larger particles are typically subject to a “Lift Force” in the fractionation capillary. The lift force pushes larger particles toward the center of the capillary. The Lift force is proportional to the ratio of particle to capillary

radii, and to the eluant average velocity. Thus, lowering the eluant average velocity along with using larger-ID fractionation capillaries reduce the lift force and extend the CHDF particle size upper limit.

Fig. 9 shows CHDF UV-detector vs. time fractionation data for a blend of 5, 1, and 0.1 micron polystyrene standards. The marker is injected about one minute after the blend. This data shows that CHDF fractionation is indeed able to fractionate particles larger than one micron. However, it is desirable to increase the fractionation resolution further in order to enhance particle size analysis capability for these larger particles. Further work is in progress.

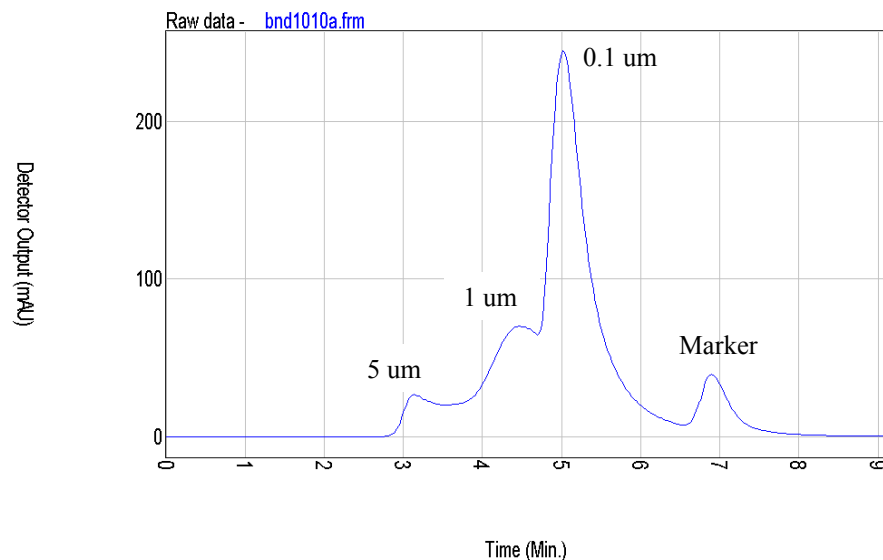


Figure 9. CHDF UV-detector raw data output for a blend of 5, 1, and 0.1 micron polystyrene latex standards. Sodium benzoate “marker” is injected about 1 minute after the blend.

On-Line Development

Today, there is a lack of (process) in-line, at-line, or on-line particle size analyzers suitable for analysis of liquid dispersions. Process particle sizers can become a vital component of slurry/dispersion/latex/emulsion production. Such analyzers can provide labor savings, as well as ensure product quality. Process particle sizers must be highly accurate, reproducible, precise, and reliable (12).

Fig. 10 shows a schematic diagram of an on-line CHDF device. The CHDF2000 unit used here is identical to the off-line device available commercially (Matec Applied Sciences, Northborough, MA). With the off-line device, samples are injected into the fractionation capillary using either an on-board manual HPLC-type injection valve or an HPLC auto-sampler. In the on-line setup, the sample flows directly from the process into an automated injection valve. The automated injection valve is actuated by the CHDF2000 on-line software in order to make sample injections every 5-10 minutes.

This particular arrangement has been used with a batch-polymerization reactor. This on-line device can also be used with continuous or semi-continuous reactors, as well as steady-state slurry streams.

The percent solids level of a batch polymerization reactor starts at zero and increases with time (13). The on-line CHDF setup must be able to handle this constant increase (CHDF analysis is typically performed in the weight-percent solids range of 0.1 to 5%). The analysis process is as follows:

A “drip” line connected to the reactor system takes a steady stream of sample through the remotely-actuated (HPLC) injection valve. The sample is diluted as needed at point D. The injection valve automatically takes samples from the drip line and performs sample injections into the CHDF fractionation capillary every few minutes. CHDF eluant continuously flows through the injection valve in order to carry the samples into the fractionation capillary. The dilution valve sets the diluent vent (Y)/dilution (D) split ratio.

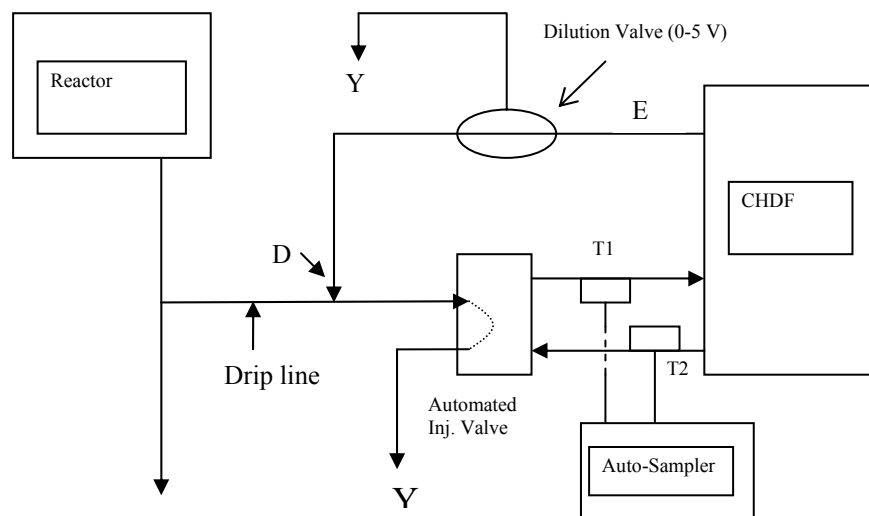


Figure 10. On-line CHDF setup equipped with sample auto-dilution.

In order to eliminate the need for a diluent pump, the effluent (E) from the CHDF is used as diluent. E is split at the dilution valve into a vented (Y), and a diluent (DFR) portion.

Valves T1 and T2 allow the use of an HPLC auto-sampler for calibration-standard analysis. The operator can thus perform periodic performance tests of the on-line CHDF setup.

The CHDF software calculates the area under each Fractogram. The dilution level is calculated by comparing the current Fractogram area to a pre-established suitable area value as follows:

$$DFR = C \cdot PA / FA \quad [2]$$

Where DFR is the diluent flow rate, C is a constant, PA is the pre-established (acceptable) Fractogram area, and FA is the sample fractogram area. DFR is set by sending a 0-5 volt signal to the dilution valve. As DFR increases, the vented (Y) eluant flow rate decreases.

PSD data files are saved to a network location. A Honeywell *PlantScape* process control system reads the PSD data and performs process control steps such as valve opening/closing and reactor temperature adjustment.

Figures 11 and 12 show polyvinyl acetate CHDF data collected from an on-line device connected to a batch reactor.

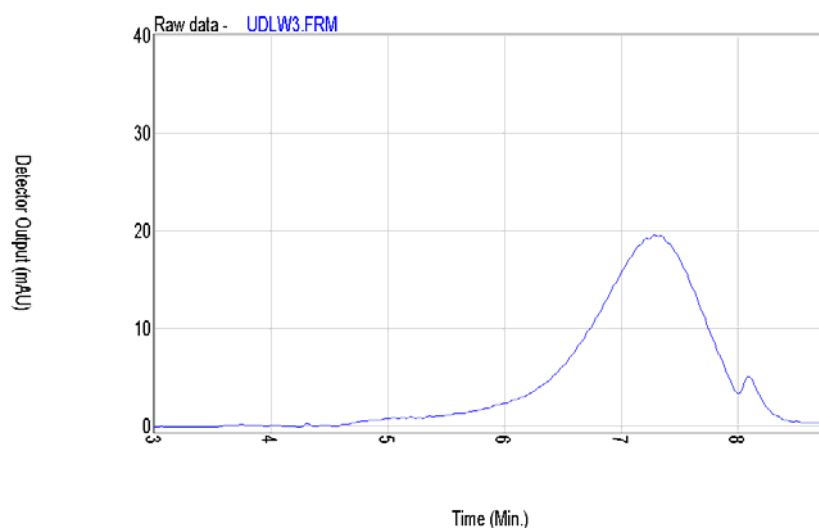


Figure 11. On-line CHDF UV-detector output for a PVA latex from a batch reactor.

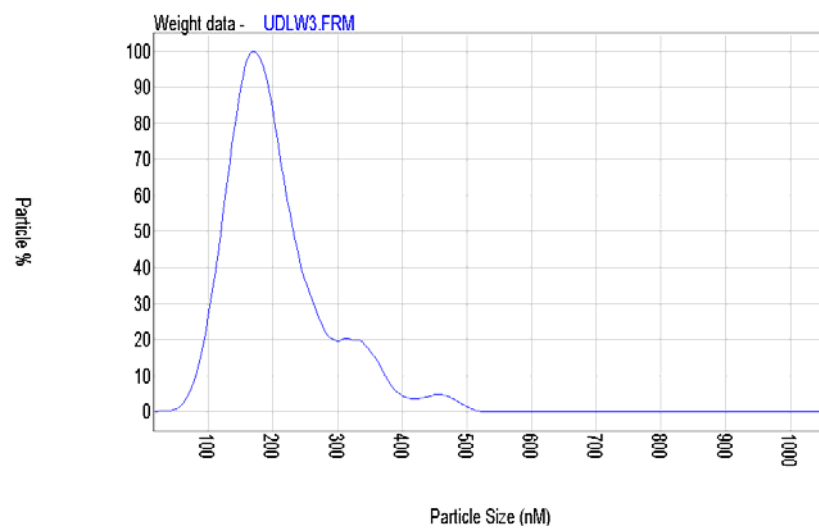


Figure 12. On-line CHDF PSD data for PVA latex from a batch reactor.

Conclusions

CHDF particle size fractionation can be used for high-resolution particle size analysis of dispersions in the particle size range of 2 nm to 5 microns. A process

on-line particle sizer has been implemented based on CHDF fractionation. This on-line device is capable of performing automatic sample dilution, and interfacing with a Honeywell Plant Control system.

Acknowledgements

The author would like to thank Dr. Tim Crowley for sharing some of the CHDF on-line data presented here.

References

1. Barth, H. G., and Flippen, R. B., *Anal. Chem.*, 67, 257R-272R, **1995**.
2. Weiner, B. B., and Tscharnuter, W. W., in *Particle Size Distribution: Assessment and Characterization*, ACS Symp. Series 332, p. 48, 1987.
3. Silebi, C. A., and DosRamos, J. G., *AIChE J.*, 35, 165, 1989.
4. DosRamos, J. G., Ph.D. Dissertation, Lehigh U., 1988.
5. www.matec.com
6. DosRamos, J. G., and Silebi, C. A., *J. Coll. Int. Sci.*, 135, 1, 1990.
7. Venkatesan, J., DosRamos, J. G., and Silebi, C. A., in *Particle Size Distribution II: Assessment and Characterization*, ACS Symp. Series 472, p. 279, 1991.
8. DosRamos, J. G., in *Particle Size Distribution III: Assessment and Characterization*, ACS Symp. Series 693, p. 207, 1998.
9. Silebi, C. A., Ph.D. Dissertation, Lehigh U., 1977.
10. Bohren, C., and Huffman, D. R., *Absorption and Scattering of Light by Small Particles*, Wiley Interscience Publication, 1983.
11. DosRamos, J. G., and Silebi, C. A., *Polym. Int.*, 30, 445, 1993.
12. Venkatesan, J., and Silebi, C. A., in *Particle Size Distribution III: Assessment and Characterization*, ACS Symp. Series 693, p. 266, 1998.
13. Dr. Tim Crowley, U. Delaware, direct communication.